Chinese Journal of Chemical Engineering 90 (2026) 333–347

Contents lists available at ScienceDirect

Chinese Journal of Chemical Engineering

journal homepage: www.elsevier.com/locate/CJChE

Full Length Article

An optimization strategy for complex distillation configurations to escape local optima and analysis of its occurrence

Chenghao Xing , Yanyang Wu *, Xiaolong Zhou *, Bin Wu , Kui Chen , Lijun Ji

School of Chemical Engineering, East China University of Science & Technology, Shanghai 200237, China

ARTICLE INFO

Article history:
Received 31 July 2025
Received in revised form
26 September 2025
Accepted 28 September 2025
Available online 31 October 2025

Keywords:
Global optimization strategy
Liquid-only transfer extractive dividing wall column
Back-mixing
Coupling
Local minima

ABSTRACT

Common optimization methods for enhanced distillation include sequential iteration methods and metaheuristic algorithms, which typically face tedious computation and are easily trapped into local minimum. Therefore, it is essential to develop a strategy that enables simultaneous evaluation of multiple solutions. In this paper, a global optimization framework integrating MATLAB and Aspen Plus for liquid-only extractive dividing wall column (LEDWC) and conventional extractive distillation (CED) systems is proposed to enhance both computational efficiency and search robustness. All possible combinations of key variables, including distillate and entrainer flow rates, feed stage, and total stage numbers, *etc.*—are considered systematically. They are arranged in full permutation within a sufficiently wide range. The permutation is then divided into multiple matrices by MATLAB. They are sequentially input into sensitivity analysis module in Aspen Plus through communication with MATLAB. Each group of integrated variables which satisfies the given constraints is used for the total annual cost (TAC) calculation. The mixture of ethanol (EtOH) and water, which can form a minimum boiling azeotrope (89.6% (mol) EtOH) at 100 kPa, is taken as a study system. Five different feed mixtures are taken for comprehensive analysis. The TAC profiles as a function of the total number of stages for the left column (N_{CL}) in the LEDWC clearly indicate that the proposed strategy successfully identified multiple local minima, demonstrating its capability to detect and escape suboptimal regions in highly nonlinear systems. The existence of local minima can be attributed to the coupling interaction between structural and process variables, as well as the influence of flow characteristics within the column. This work indicates that as N_{CL} increases, there is a competitive effect between the decrease in reflux ratio for the left column (RR_{CL}) and the increase in reboiler temperature, leading to fluctuations in energy consumption; while changes in the distillation flow rate for the left column cause nonlinear changes in RR_{CL} and the liquid flow rate between the left and right columns, further promoting the emergence of multiple local minima during the TAC optimization process. Additionally, analysis of the flow characteristics within the column revealed that the back-mixing phenomenon commonly observed in CED is absent in LEDWC, suggesting that back-mixing may be an important factor contributing to the more frequent occurrence of local optima.

1. Introduction

The optimal design of enhanced distillation columns involves multiple manipulated variables [1], resulting in a nonlinear programming problem [2,3]. There are two major strategies, which are the sequential iteration methods and meta-heuristic algorithms [4–6]. The former optimizes variables consecutively with some parameters being fixed, which neglect the other options, in order to enhance computational efficiency. Cui *et al.* [7] manipulated product purities through reflux ratios with fixed distillate flow rates utilizing sequential iteration method. It didn't consider the effects of distillate flow rates. Li *et al.* [8] incorporated distillate flow rates into consideration. However, the extractive distillation column (EDC) was optimized under the fixed conditions of entrainer recovery column (ERC) in this process. As sequential iteration simplifies the process by optimizing variables in a fixed order, it is limited by its inability to explore the entire feasible domain, often leading to suboptimal solutions.

In contrast, meta-heuristic algorithms can be more effective in achieving optimal solutions. Liu *et al.* [9] incorporated chaotic

* Corresponding authors.
E-mail addresses: wyywitty@ecust.edu.cn (Y. Wu), xiaolong@ecust.edu.cn (X. Zhou).

https://doi.org/10.1016/j.cjche.2025.09.020

sequences into differential evolutionary algorithms to generate ergodic variables, thereby enhancing optimization efficiency and reducing the likelihood of local solutions. Compared to the conventional differential evolution algorithm, the improved algorithm avoids prolonged stagnation during optimization, indicating a stronger capability to escape local optima. He *et al.* [10] provided a novel optimization approach based on the NSGA-II algorithm, a multi-objective method that simultaneously optimizes total annual cost (TAC), carbon emissions, and thermodynamic efficiency. The purpose of this approach is to prevent the optimization from converging to local optima. It is achieved through population-based search, non-dominated sorting, and crowding distance mechanisms, which enhance global exploration and maintain solution diversity as well. Ma *et al.* [11] introduced a hybrid approach that integrates equation-oriented methods with genetic algorithms for the optimization of dividing wall column (DWC) systems. The convergence is improved by permitting larger simulation tolerances when divergence occurs under stricter settings. It reduced TAC by more than 10% compared to sequential iteration methods.

However, the monolithic structure of these meta-heuristic algorithms still imposes limitations on flexibility and adaptability, particularly when addressing large-scale, strongly coupled optimization problems. To address the limitations of conventional monolithic algorithm structures, recent research has increasingly focused on modular optimization frameworks. Ramírez *et al.* [12] provided flexible, component-based structure that facilitates the embedding of diverse objective functions and evolutionary strategies, offering improved adaptability for multi-objective chemical process optimization tasks. Cai *et al.* [13] proposed a cooperative metaheuristic algorithm based on heterosis theory, which incorporates a subpopulation structure and a search–escape–synchronize module. This modular strategy enhances both global exploration and local exploitation capabilities, significantly reducing the risk of premature convergence. Similarly, Beck *et al.* [14] developed the Paddy evolutionary algorithm, in which biologically inspired modules (seeding, selection, and sowing) collectively guide the search process. The modular design improves population diversity and convergence stability while avoiding direct dependence on the objective function during early search stages. These studies highlight the advantages of modular strategy integration in enhancing search robustness, promoting candidate diversity, and accelerating convergence.

Currently, most meta-heuristic algorithms for distillation columns still rely on a systematic, point-by-point evaluation of each solution within the entire search space [9]. This results in significantly increased computational costs when dealing with highly coupled variables or large-scale design problems [15,16]. Therefore, it is necessary to develop optimization modules capable of simultaneously evaluating multiple candidate solutions and integrating seamlessly with meta-heuristic algorithms.

In this study, a novel modular optimization strategy that can be integrated into broader algorithmic frameworks. Is proposed to enhance the efficiency of distillation column design and overcome the limitations associated with local minimum in highly nonlinear systems. A systematic analysis of various combinations of key decision variables is performed through integrated communication between MATLAB and Aspen Plus, enabling efficient global exploration of the design space. In addition, the influence of variable coupling on local minima is investigated. To validate the effectiveness of the proposed optimization strategy, the liquid-only extractive dividing-wall column (LEDWC) is selected as the case study. The strategy is also applied to the conventional extractive distillation (CED), and the occurrence of local minima is comparatively analyzed for both configurations.

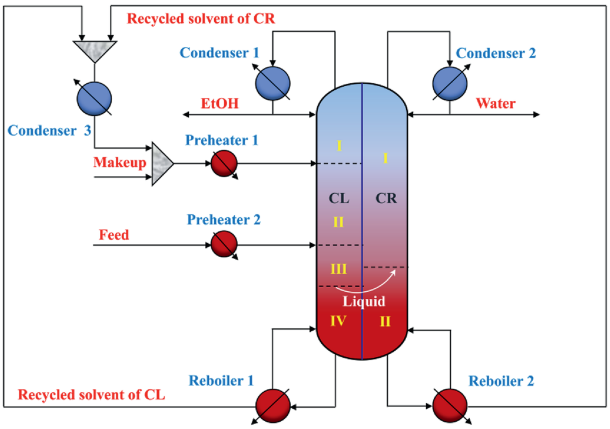

Fig. 1. Schematic diagram of LEDWC.

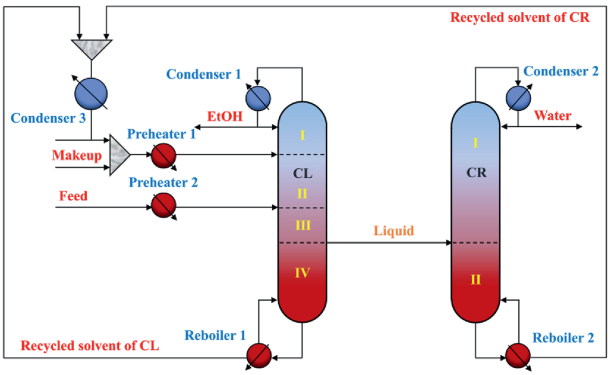

Fig. 2. The equivalent model of LEDWC.

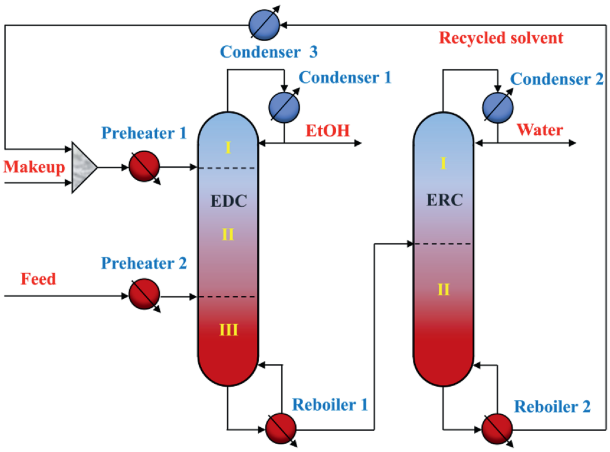

Fig. 3. Schematic diagram of CED.

Table 1
The price of heat steam.

Steam pressure/Pa	Latent heat of vaporization/kJ·kg^{-1}	Price/USD·GJ^{-1}	Temperature/K
2.5×10^5	2147.26	7.11	412.14
6.4×10^5	2057.85	7.51	440.43
2.3×10^6	1849.46	8.47	494.98

Table 2
The specific ranges for each variable in LEDWC.

EtOH/water molar ratio		10/90	30/70	50/50	70/30	90/10
N_{CL}	Lower bound	18	18	18	18	18
	Upper bound	65	65	65	65	65
N_{CR}	Lower bound	8	8	8	8	8
	Upper bound	40	40	40	40	40
$N_{F\text{-}E\text{-}CL}$	Lower bound	2	2	2	2	2
	Upper bound	10	10	10	10	10
$N_{F\text{-}CL}$	Lower bound	$N_{F\text{-}E\text{-}CL}+1$	$N_{F\text{-}E\text{-}CL}+1$	$N_{F\text{-}E\text{-}CL}+1$	$N_{F\text{-}E\text{-}CL}+1$	$N_{F\text{-}E\text{-}CL}+1$
	Upper bound	$N_{CL}-2$	$N_{CL}-2$	$N_{CL}-2$	$N_{CL}-2$	$N_{CL}-2$
$N_{F\text{-}L\text{-}CL}$	Lower bound	$N_{F\text{-}CL}+1$	$N_{F\text{-}CL}+1$	$N_{F\text{-}CL}+1$	$N_{F\text{-}CL}+1$	$N_{F\text{-}CL}+1$
	Upper bound	$N_{CL}-1$	$N_{CL}-1$	$N_{CL}-1$	$N_{CL}-1$	$N_{CL}-1$
$N_{F\text{-}CR}$	Lower bound	2	2	2	2	2
	Upper bound	$N_{CR}-1$	$N_{CR}-1$	$N_{CR}-1$	$N_{CR}-1$	$N_{CR}-1$
D_{CL}/kmol·h^{-1}	Lower bound	9	29	49	69	89
	Upper bound	11	31	51	71	91
$F_{S\text{-}LEDWC}$/kmol·h^{-1}	Lower bound	5	10	15	20	30
	Upper bound	20	25	40	55	70
D_{CR}/kmol·h^{-1}	Lower bound	89	69	49	29	9
	Upper bound	91	71	51	31	11
D_L/kmol·h^{-1}	Lower bound	100 × (1-molar ratio)	100 × (1− molar ratio)	100 × (1− molar ratio)	100 × (1− molar ratio)	100 × (1− molar ratio)
	Upper bound	$100+F_{S\text{-}LEDWC}-D_{CL}$	$100+F_{S\text{-}LEDWC}-D_{CL}$	$100+F_{S\text{-}LEDWC}-D_{CL}$	$100+F_{S\text{-}LEDWC}-D_{CL}$	$100+F_{S\text{-}LEDWC}-D_{CL}$

Table 3
The specific ranges for each variable in CED.

EtOH/water molar ratio		10/90	30/70	50/50	70/30	90/10
N_{EDC}	Lower bound	18	18	18	18	18
	Upper bound	65	65	65	65	65
N_{ERC}	Lower bound	8	8	8	8	8
	Upper bound	40	40	40	40	40
$N_{F\text{-}E\text{-}EDC}$	Lower bound	2	2	2	2	2
	Upper bound	10	10	10	10	10
$N_{F\text{-}EDC}$	Lower bound	$N_{F\text{-}E\text{-}EDC}+1$	$N_{F\text{-}E\text{-}EDC}+1$	$N_{F\text{-}E\text{-}EDC}+1$	$N_{F\text{-}E\text{-}EDC}+1$	$N_{F\text{-}E\text{-}EDC}+1$
	Upper bound	$N_{EDC}-2$	$N_{EDC}-2$	$N_{EDC}-2$	$N_{EDC}-2$	$N_{EDC}-2$
$N_{F\text{-}ERC}$	Lower bound	2	2	2	2	2
	Upper bound	$N_{ERC}-1$	$N_{ERC}-1$	$N_{ERC}-1$	$N_{ERC}-1$	$N_{ERC}-1$
D_{EDC}/kmol·h^{-1}	Lower bound	9	29	49	69	89
	Upper bound	11	31	51	71	91
D_{ERC}/kmol·h^{-1}	Lower bound	89	69	49	29	9
	Upper bound	91	71	51	31	11
$F_{S\text{-}CED}$/kmol·h^{-1}	Lower bound	5	10	15	20	30
	Upper bound	20	25	40	55	70

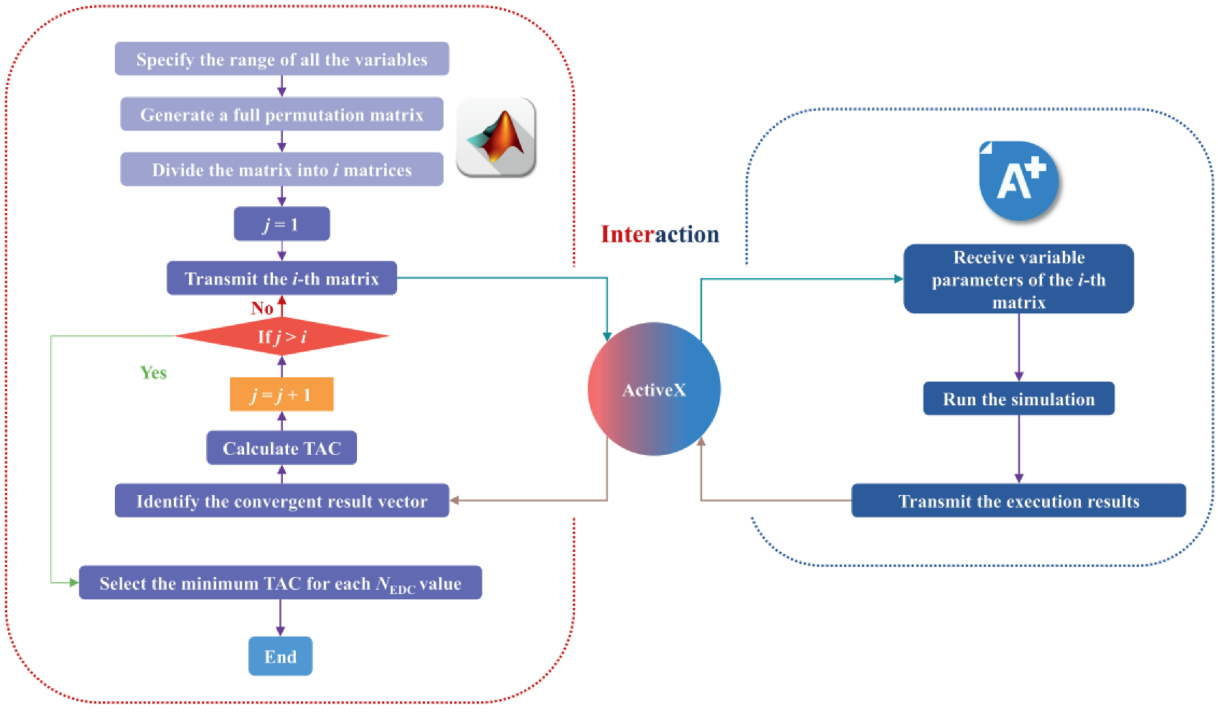

Fig. 4. The global optimization framework.

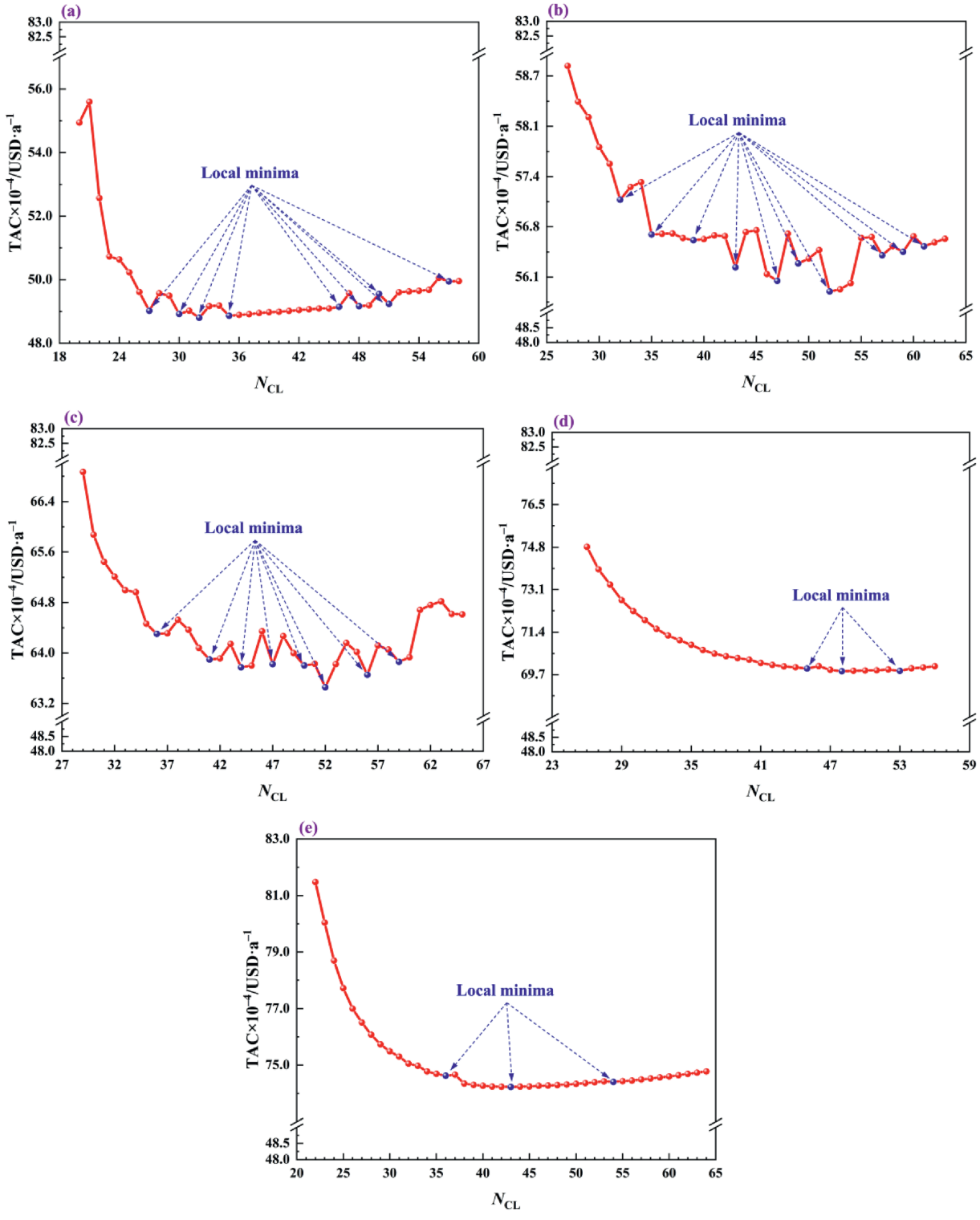

Fig. 5. The global optimizations for the TAC of LEDWC at different EtOH/water feed molar ratios: (a) = 10/90, (b) 30/70, (c) 50/50, (d) 70/30, and (e) 90/10.

2. Simulation

The separation of the ethanol (EtOH)–water mixture, which forms a minimum-boiling azeotrope at 100 kPa with an EtOH concentration of 89.6% (mol), is taken as the study case in this paper. Ethylene glycol (EG) is selected as the entrainer for the extractive distillation (ED) process [17–19]. The physical properties of the mixture are provided in Table S1 (in Supplementary Material) [20–22]. Steady-state simulations are carried out using Aspen Plus V11 software.

The vapor–liquid equilibrium data are obtained from the literatures [23–25]. It is correlated using the non-random two-liquid

(NRTL) model. As shown in Fig. S1, the correlation and experimental data can be matched well. Therefore, the NRTL equation is taken for all the subsequent simulations.

2.1. LEDWC configuration

LEDWC has evolved from extractive dividing wall column (EDWC), offering the advantages of energy saving over traditional extraction methods, as well as enhanced single-column controllability compared to EDWC. Demonstrating strong engineering feasibility and commercial potential, it is expected to find broader application in the future. The LEDWC designed for the separation of the azeotrope is illustrated in Fig. 1. A vertically continuous partition wall divides the LEDWC into the left column and right column, labeled CL and CR, respectively. There is a liquid-only transfer stream between the CL and CR. This stream divides the section below the EtOH–water mixture feed location into two parts, effectively removing water and a portion of EG early on, which are then directed to CR for further separation. Ultimately, EtOH and water are drawn as products at the top of the CL and CR, respectively, while EG is recycled from the reboilers in both sections. The LEDWC equivalent model is developed using the RadFrac model in Aspen Plus, as shown in Fig. 2. Heat transfer through the continuous partition wall is not considered in this model.

The pressures on each side of the LEDWC are left out of optimization. The optimization for LEDWC involves six structural variables and six process variables. The structural variables include the total number of stages for CL and CR (N_{CL} and N_{CR}), the feed and entrainer stages for CL ($N_{F\text{-}CL}$ and $N_{F\text{-}E\text{-}CL}$), the liquid stream withdrawal stage for CL ($N_{F\text{-}L\text{-}CL}$) and feed stage for CR($N_{F\text{-}CR}$). Moreover, the process variables are two reflux ratios for CL and CR (RR_{CL}, RR_{CR}), the distillate flow rates for CL and CR (D_{CL}, D_{CR}), the liquid stream flow rate between CL and CR (D_L), and the feed flow rate of the entrainer ($F_{S\text{-}LEDWC}$).

2.2. CED configuration

CED typically involves two columns, consisting of the EDC and ERC. The EDC primarily realizes the separation of components in the feed, while the ERC deals with the recovery of the entrainer. In this study, EG serves as the entrainer and is preheated before being introduced into the stage near the top of the EDC. Concurrently, the EtOH–water mixture is preheated and fed into the stage near the bottom of the EDC. This configuration ensures the relative volatility between the key components being adjusted along the whole column, thereby achieving effective separation, as illustrated in Fig. 3.

The optimization for CED involves five structural variables and five process variables. The structural variables include the total number of stages for EDC and ERC (N_{EDC} and N_{ERC}), the feed and entrainer stages for EDC ($N_{F\text{-}EDC}$ and $N_{F\text{-}E\text{-}EDC}$), and feed stage for ERC ($N_{F\text{-}ERC}$). Additionally, the process variables comprise two reflux ratios for EDC and ERC (RR_{EDC} and RR_{ERC}), two distillation flow rates for EDC and ERC (D_{EDC} and D_{ERC}), and the entrainer feed flow rate ($F_{S\text{-}CED}$).

2.3. Constraints and optimization objectives

In this study, the LEDWC and CED are operated at 100 kPa with a stage pressure drop of 0.6868 kPa. Five EtOH–water feed combinations are considered. The corresponding molar ratios (EtOH/water) are as follows: 10/90, 30/70, 50/50, 70/30 and 90/10. The fresh feed and entrainer, maintained at 303.15 K, is preheated to reach a saturated liquid state, with an overall flow rate of 100 $kmol \cdot h^{-1}$. The recycled entrainer is cooled down to 303.15 K. The purities of EtOH and water are set at 99.5% (mol) and the purity of the recycled entrainer is at least 99.99% (mol). The TAC minimization is taken as the objective function. It can be calculated by Eq. (1) [26]:

$$\mathrm{TAC} = \text{Operating cost} + \frac{\text{Capital cost}}{\text{Payback year}} \tag{1}$$

where the operating cost consists of heat steam and cooling water, and the price of cooling water is 0.354 ($USD \cdot kW^{-1} \cdot h^{-1}$) [27], the price of heat steam is determined by the Trouble Less Valve system and listed in Table 1 [28]; the capital cost is estimated by the total installment cost including column shells and trays, heat exchangers, *etc.* [29]; a payback period of 10 years is assumed, with an operating time of 8000 h every year [30]. The detailed equations for calculating the operating and capital cost are presented in the Supplementary Material.

2.4. Optimization procedure

To achieve global optimization, the optimization process is based on the communication between MATLAB and Aspen Plus. The reflux ratio is specified by the design specification module to achieve control over product purity. For the other variables, MATLAB generates multiple data matrices containing different variable values within the specific ranges of the variables. The variable specific ranges under different feed conditions for LEDWC and CED are listed in Tables 2 and 3, respectively.

The data matrices are sequentially transmitted to Aspen Plus *via* an ActiveX server for sensitivity analysis. MATLAB monitors Aspen Plus's operational status at 2-s intervals to check the completion of computations and detect all the system-related interruptions. Simulation results vectors that satisfy the constraints are selected from Aspen Plus, and then the TAC is

Table 4
The LEDWC optimized variables and corresponding TAC values at different feed molar ratios of EtOH/water.

	10/90	30/70	50/50	70/30	90/10
N_{CL}	32	52	52	48	43
N_{CR}	21	21	15	18	12
$N_{F\text{-}E\text{-}CL}$	4	4	4	4	4
$N_{F\text{-}CL}$	19	42	42	35	33
$N_{F\text{-}L\text{-}CL}$	27	47	47	43	41
$N_{F\text{-}CR}$	5	3	8	6	4
D_{CL}/$kmol \cdot h^{-1}$	9.78	29.94	50.03	70.23	90.42
$F_{S\text{-}LEDWC}$/$kmol \cdot h^{-1}$	9.90	13.00	22.10	37.00	47.10
D_{CR}/$kmol \cdot h^{-1}$	90.40	70.21	50.00	29.80	9.60
D_L/$kmol \cdot h^{-1}$	98.00	80.20	69.90	61.10	55.00
TAC/$USD \cdot a^{-1}$	488007	559093	634546	698340	742257

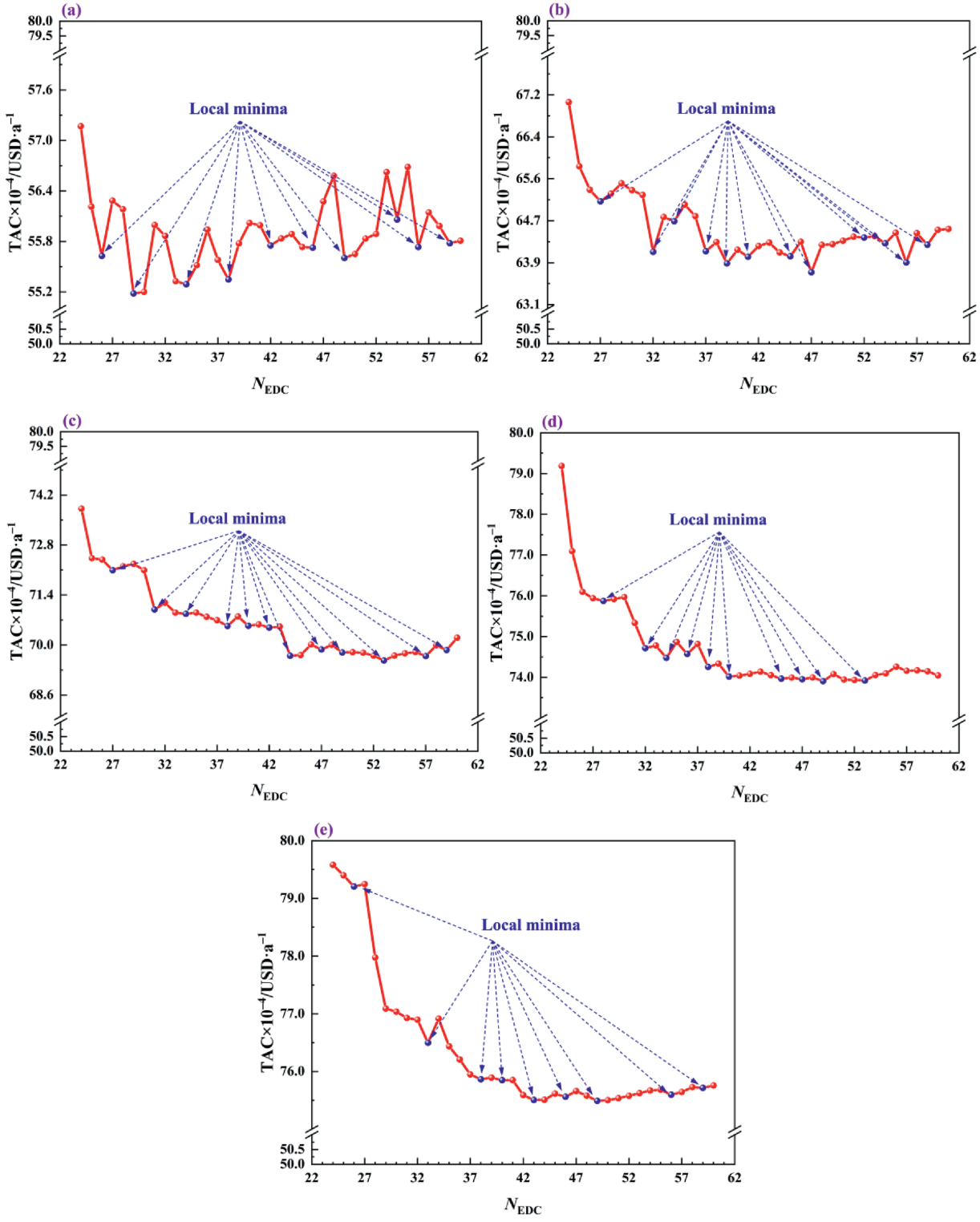

Fig. 6. The global optimizations for the TAC of CED at different EtOH/water feed molar ratios: (a) 10/90, (b) 30/70, (c) 50/50, (d) 70/30, and (e) 90/10.

calculated by MATLAB. The vector corresponding to the minimum TAC is identified and recorded accordingly. The global optimization process is shown in Fig. 4. To improve computational efficiency, this study uses a multi-threading method for parallel computing, with each thread assigned a fixed N_{CL} or N_{EDC} value for optimization. The entire computation is performed on a 64-bit Windows 10 operating system equipped with a 2.6 GHz AMD EPYC 7Y43 48-core processor and 32.0 GB of RAM.

3. Results and Discussion

3.1. Optimization results

The optimization results for LEDWC are shown in Fig. 5, with the specific optimized values for each variable listed in Table 4. They all fall within the variable ranges specified, and no variables reach their extreme values. Significant differences in TAC are

observed under different feed conditions, primarily due to the increasing difficulty of separation. The curves overall exhibit a trend of first decreasing and then increasing, indicating that there is a minimum TAC value under each feed condition. For EtOH/water feed molar ratios of 10/90, 30/70, 50/50, 70/30 and 90/10, the corresponding minimum TAC values are 488007, 559093, 634546, 698340, and 742257 USD·a^{-1}, respectively. In addition, it clearly identifies multiple local optima, indicating that the proposed optimization module has good global search capabilities and can effectively escape local optima to achieve better optimization results.

The optimization results for CED are shown in Fig. 6, with the specific optimized values for all variables listed in Table 5. The value results also show that no variables reach their extreme values. The overall trend is similar to the optimization results for LEDWC. For EtOH/water feed molar ratios of 10/90, 30/70, 50/50, 70/30 and 90/10, the corresponding minimum TAC values are 551823, 637197, 695667, 739048, and 754913 USD·a^{-1}, respectively.

To further validate the feasibility of the global optimization method proposed in this study, the same feed conditions as those in the literature (EtOH/water feed molar ratios of 85/15) were selected for optimization. During the optimization process, consistent with the literature, no preheating treatment is applied to the CED feed. The optimization results are shown in Fig. 7. The literature employed a sequential iterative method, achieving a TAC of 587394 USD·a^{-1} [31], whereas the optimization method used in this study resulted in a TAC of 575951 USD·a^{-1}. This indicates that the proposed strategy has stronger global search capabilities and can effectively escape local optima.

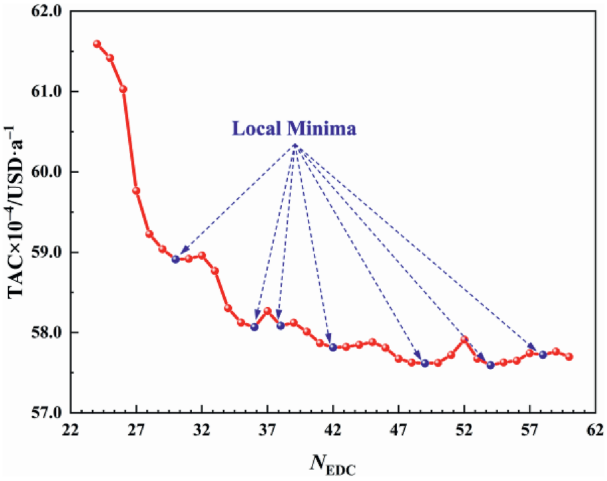

Fig. 7. The global optimization for the TAC of CED at feed molar ratio of EtOH/water = 85/15.

3.2. Local minima analysis

This section analyzes the impact of selected structural and process variables of the LEDWC on the occurrence of local minima. The results for the CED system are mainly shown in the Supplementary Material.

3.2.1. Structural variables

The effect of N_{CL} on the performance of the LEDWC is analyzed in this section. The variations in energy consumption, RR_{CL}, and the reboiler temperature of the CL during the optimization process are illustrated in Fig. 8. The results indicate that energy consumption, similarly to the TAC, fluctuates with changes in the number of stages, exhibiting multiple local minima. As the number of N_{CL} increases, the RR_{EDC} tends to decrease, thereby reducing the energy consumption of reboiler. However, due to pressure drops within the column and changes in the bottom composition during the optimization, the reboiler temperature rises, which in turn increases the energy consumption of reboiler. The interplay between these opposite effects results in fluctuating energy consumption of reboiler, characterized by multiple local minima, ultimately contributing to the presence of multiple local minima in the TAC during the optimization.

3.2.2. Process variables

This section investigates the impact of D_{CL} on LEDWC performance. As D_{CL} varies, RR_{CL} is adjusted accordingly to meet product purity requirements; simultaneously, D_L is dynamically regulated to ensure the convergence of the simulation process. The trends in TAC, RR_{CL}, and D_L during the optimization process are illustrated in Fig. 9. It can be observed that RR_{CL} increases with the increase in D_{CL}, indicating that the energy consumption of CL also increases; however, the changes in D_L are irregular, suggesting that the energy consumption of CR exhibits fluctuating changes. Ultimately, this instability in energy consumption leads to the appearance of multiple local minima in TAC as D_{CL} varies.

These observations not only reveal the underlying nonlinear behavior contributing to local optima in TAC but also demonstrate that the proposed strategy can capture such local minima, highlighting its effectiveness in escaping suboptimal regions and improving global search reliability.

3.2.3. Back-mixing

From the curves of TAC and N_{CL}, the local optimum value of LEDWC is slightly lower than that of CED. To explore the reasons behind this, this study further analyzes the effects of the two structures, LEDWC and CED, on the flow behavior inside the column.

Table 5
The CED optimized variables and corresponding TAC values at different feed molar ratios of EtOH/water.

	10/90	30/70	50/50	70/30	90/10
N_{EDC}	29	47	53	49	49
N_{ERC}	18	24	24	30	24
$N_{F\text{-}E\text{-}EDC}$	3	6	5	4	5
$N_{F\text{-}EDC}$	21	39	45	39	39
$N_{F\text{-}ERC}$	6	9	6	9	3
D_{EDC}/kmol·h^{-1}	9.81	29.91	50.01	70.35	90.45
D_{ERC}/kmol·h^{-1}	90.41	70.20	50.00	29.80	9.60
$F_{S\text{-}CED}$/kmol·h^{-1}	8.00	15.00	23.00	35.00	46.00
TAC/USD·a^{-1}	551823	637197	695667	739048	754913

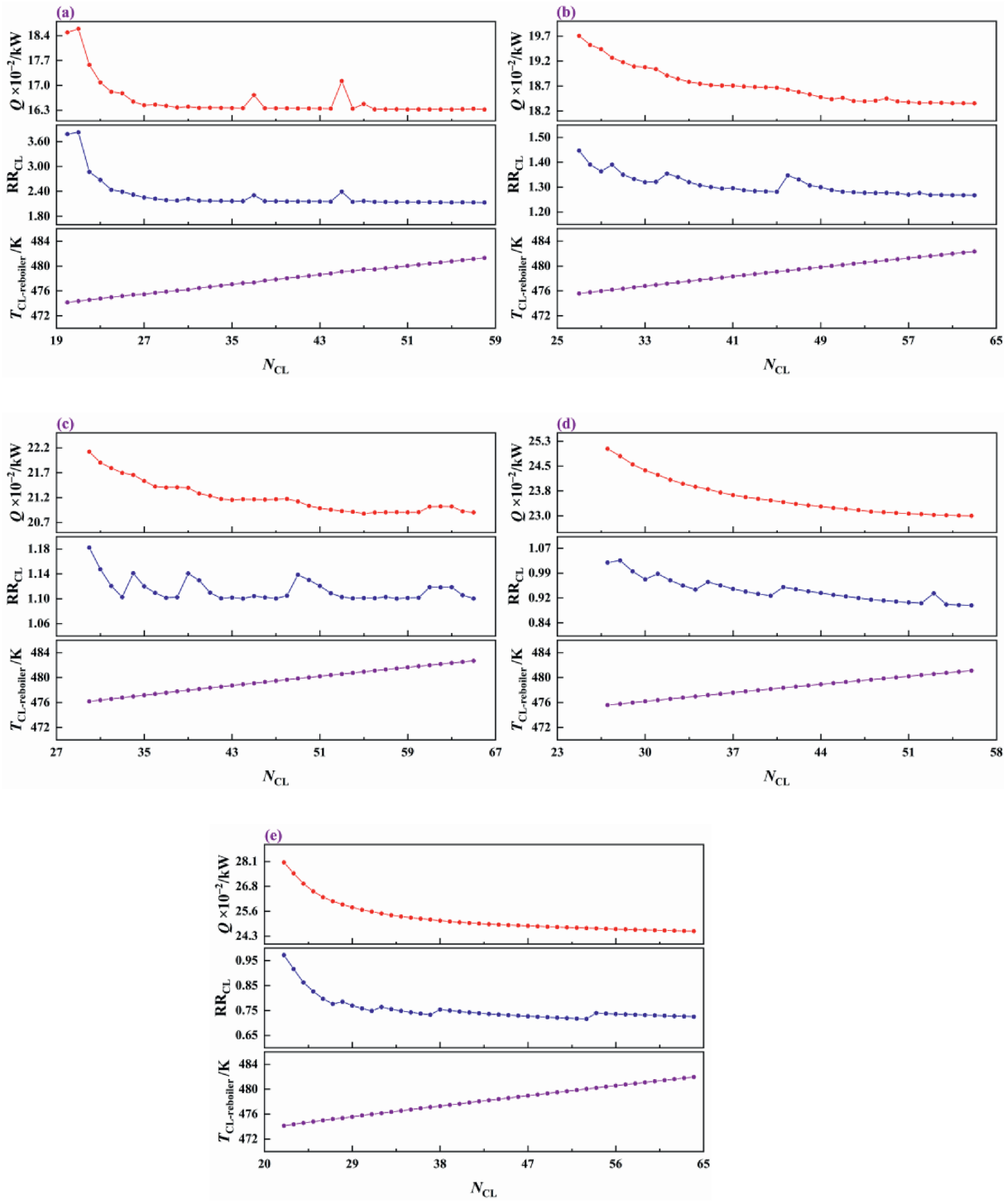

Fig. 8. The total energy consumption, RR_{CL} and the temperature of the reboiler in CL for the optimized LEDWC with varying N_{CL} at different EtOH/water feed molar ratios: (a) 10/90, (b) 30/70, (c) 50/50, (d) 70/30, and (e) 90/10.

The composition profiles within the optimized CED are illustrated in Figs. 10 and 11. Different components in EDC and ERC exhibit different curves. For the EDC, above the $N_{F\text{-}E}$, EtOH is continuously withdrawn at the top of EDC; consequently, the mole fraction of EtOH decreases gradually from the top of EDC downward to the $N_{F\text{-}E}$, while the mole fraction of water correspondingly increases; at the $N_{F\text{-}E}$, the introduction of EG causes a sudden rise in the mole fraction of EG; between the $N_{F\text{-}E}$ and the $N_{F\text{-}EDC}$, both the mole fraction of EtOH and EG gradually decrease, whereas the mole fraction of water continues to increase; at the $N_{F\text{-}EDC}$, the addition of fresh feed causes both the mole fraction of EtOH and water to rise again; from the $N_{F\text{-}EDC}$ toward the bottom of ERC, the mole fraction of EtOH initially exhibits a minor peak and then declines at the bottom due to the specification. The mole fraction of EG first decreases at the bottom and subsequently increases, while the mole fraction of

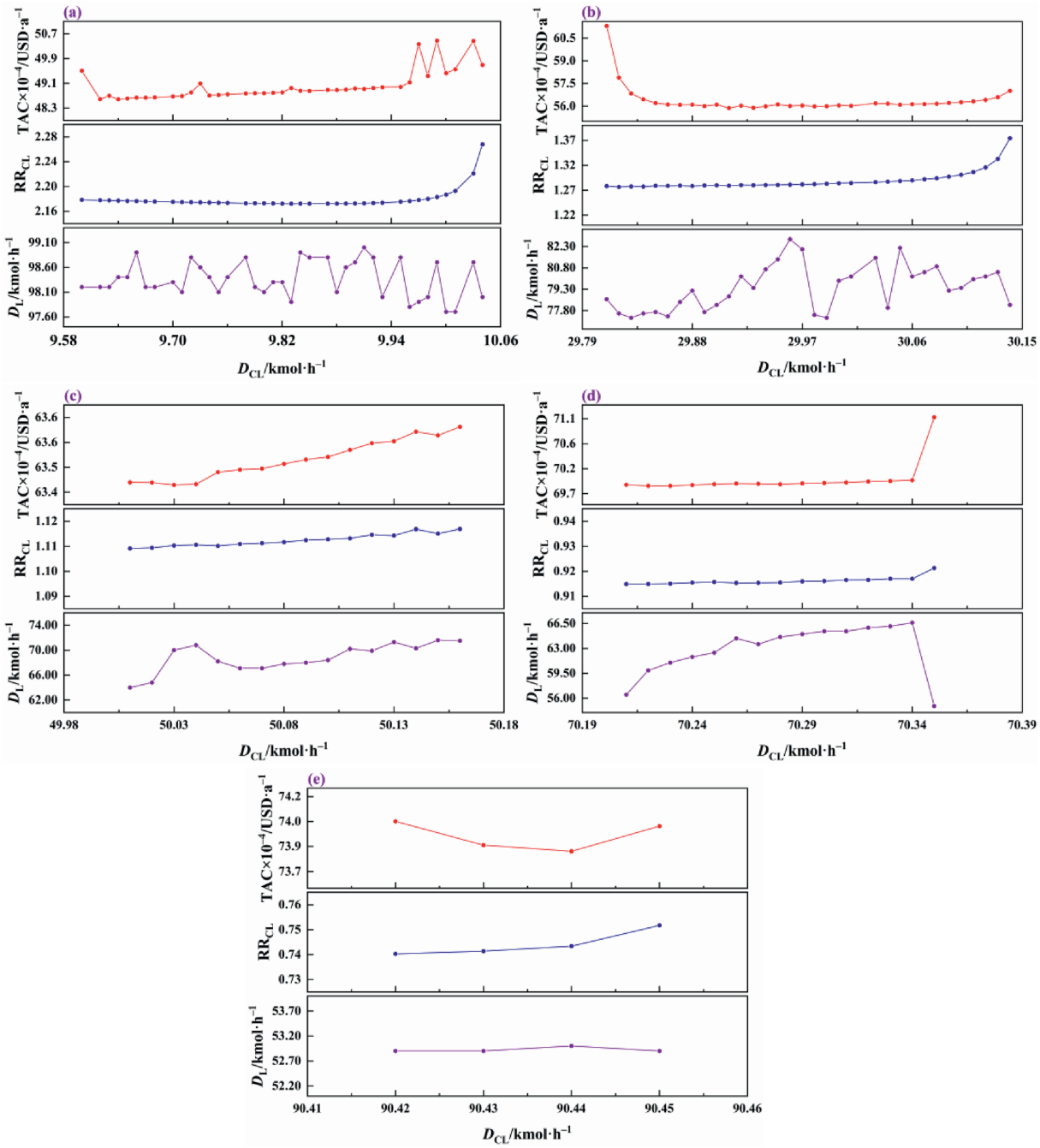

Fig. 9. The TAC, RR_{CL} and D_L for the optimized LEDWC with varying D_{CL} at different EtOH/water feed molar ratios: (a) 10/90, (b) 30/70, (c) 50/50, (d) 70/30, and (e) 90/10.

water initially rises and then decreases after reaching its peak. These composition profiles indicate the presence of back-mixing within the EDC. Finally, water, as the intermediate component, exhibits back-mixing at stages 28, 46, 52, 47, and 47 under different feed ratios, respectively. It may increase energy consumption to achieve effective separation and potentially result in the more local minimum.

The binary mixture composed of water and EG enters the ERC, where water is withdrawn at the top of the ERC. The mole fraction of water decreases smoothly along the column. The inverse occurs for EG. It indicates that no back-mixing phenomenon caused by concentration peaks occurs within the ERC.

The optimized LEDWC concentration profiles are shown in Figs. 12 and 13**.** In comparison with CED, no obvious concentration peaks appear in the distillation section of LEDWC. It indicates that there is no back-mixing, which obviously contributes to reducing the energy consumption. Meanwhile, since the composition along the column in LEDWC changes monotonously, the coupling effects between variables weaken. It results in a smoother curve of TAC variation with NCL and then reduces the probability of encountering local optima.

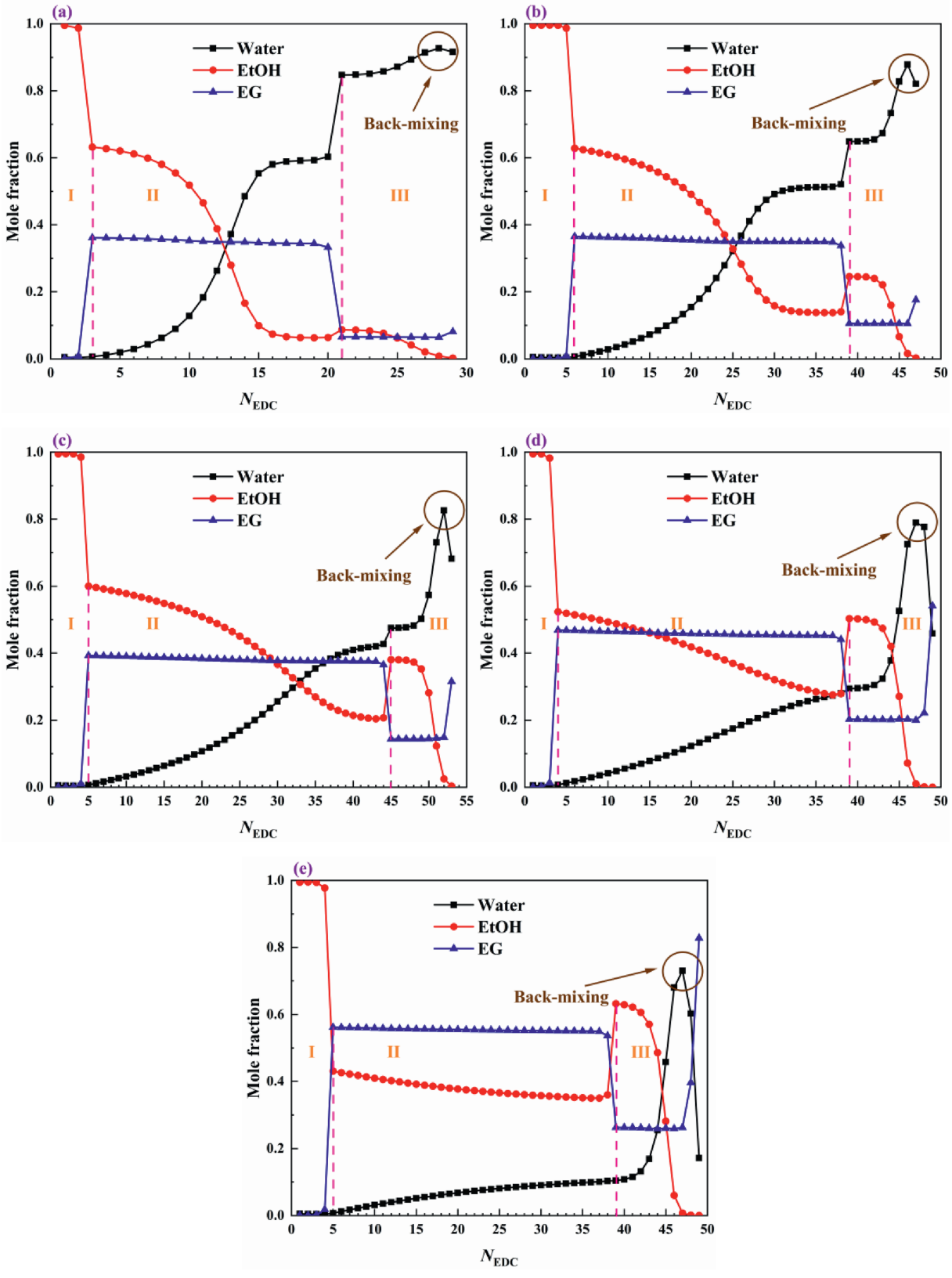

Fig. 10. The concentration distributions for the EDC of the optimized CED at different EtOH/water feed molar ratios: (a) 10/90, (b) 30/70, (c) 50/50, (d) 70/30, and (e) 90/10.

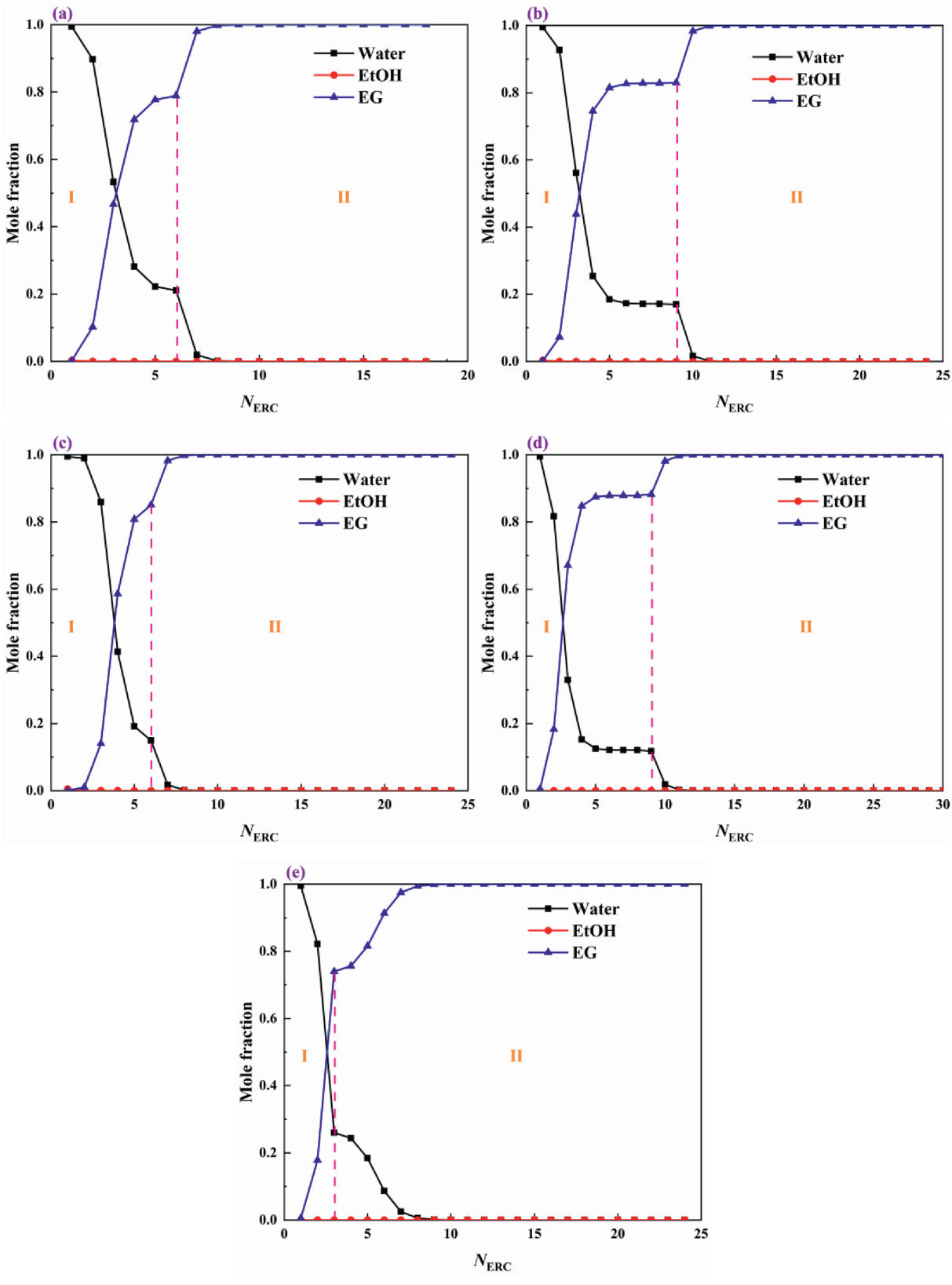

Fig. 11. The concentration distributions for the ERC of the optimized CED at different EtOH/water feed molar ratios: (a) 10/90, (b) 30/70, (c) 50/50, (d) 70/30, and (e) 90/10.

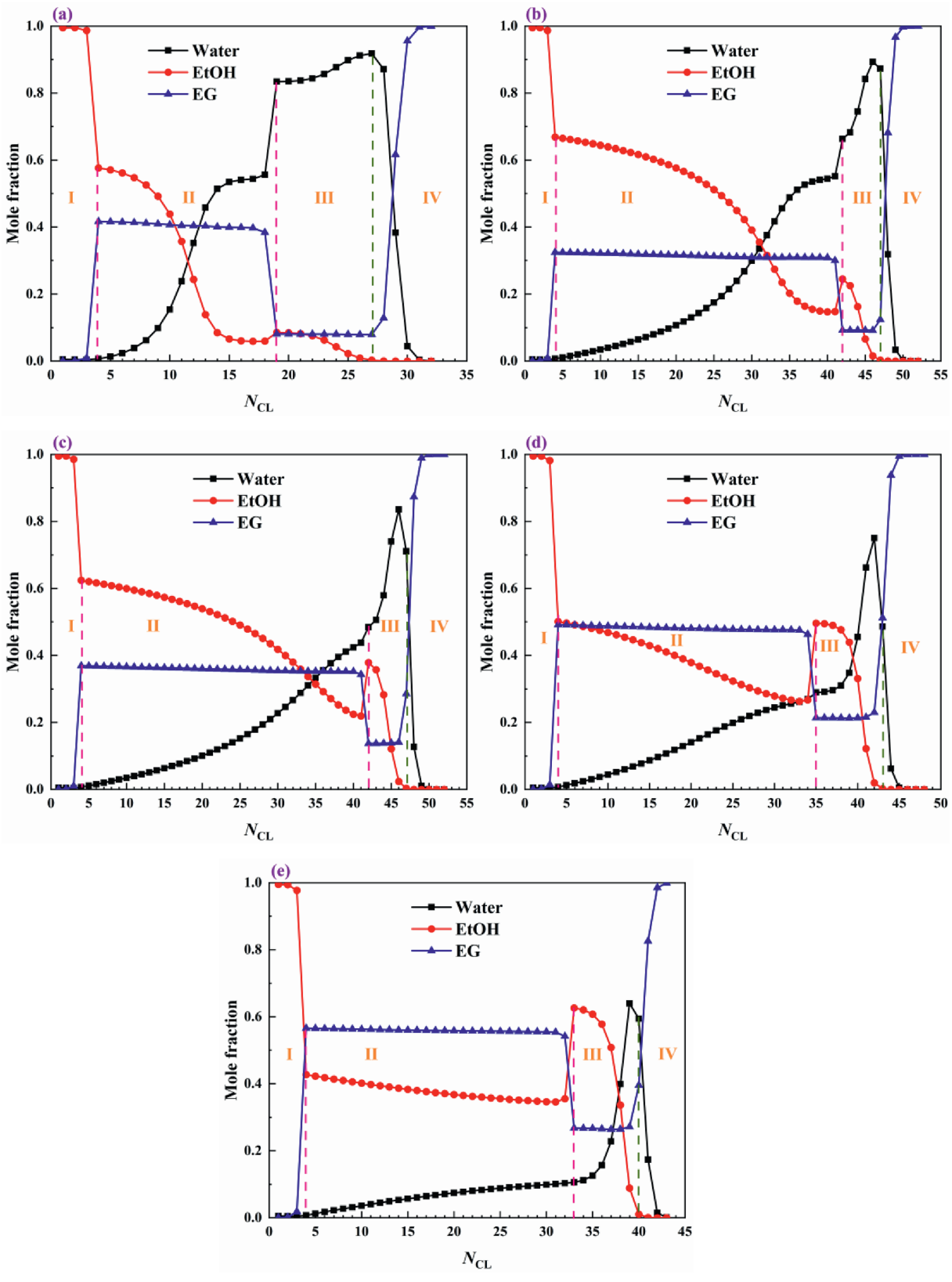

Fig. 12. The concentration distributions for the CL of the optimized LEDWC at different EtOH/water feed molar ratios: (a) 10/90, (b) 30/70, (c) 50/50, (d) 70/30, and (e) 90/10.

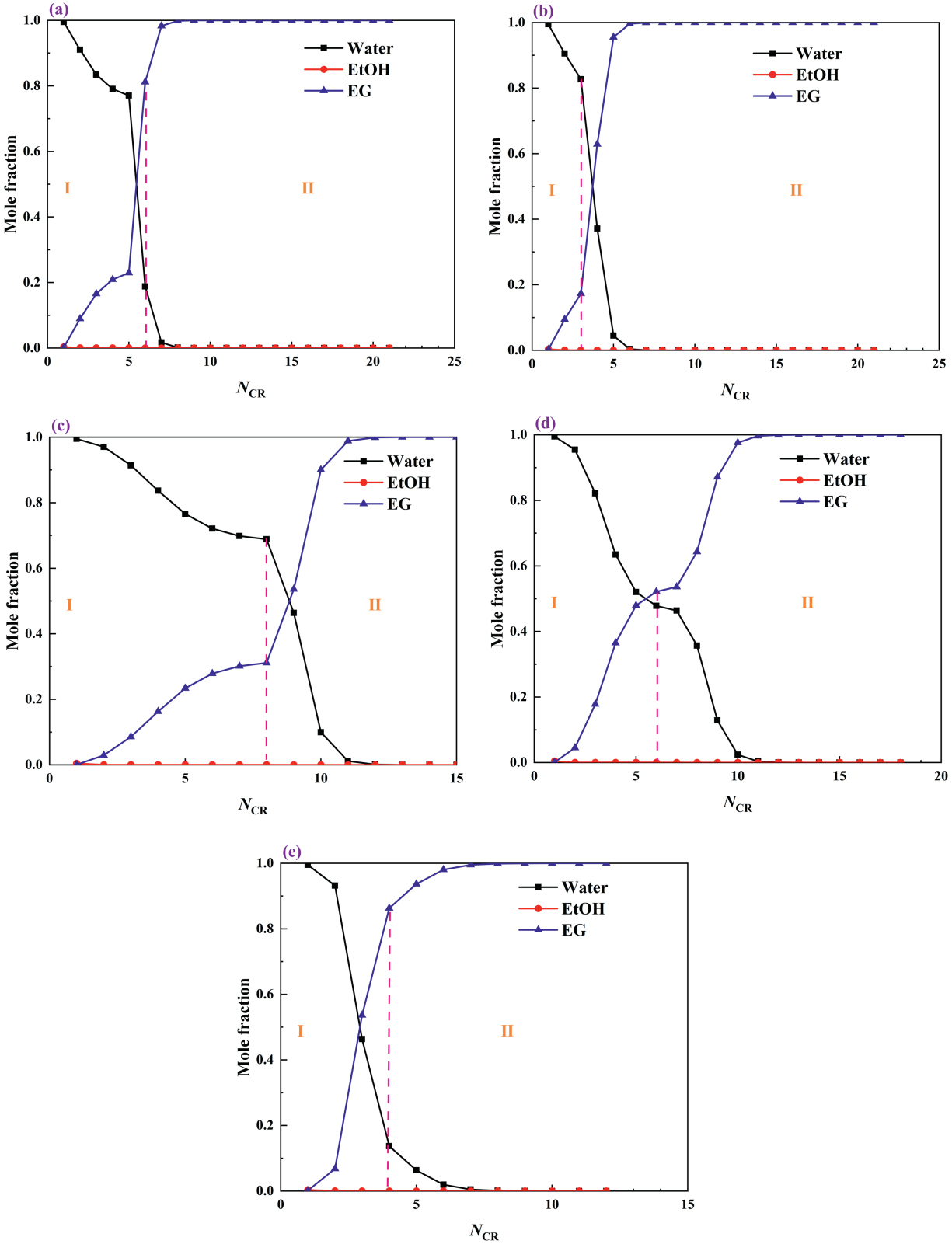

Fig. 13. The concentration distributions for the CR of the optimized LEDWC at different EtOH/water feed molar ratios: (a) 10/90, (b) 30/70, (c) 50/50, (d) 70/30, and (e) 90/10.

4. Conclusions

In this study, a novel modular optimization strategy is proposed for the nonlinear problems in the optimization of distillation columns. It effectively solves the limitations of conventional methods, which are prone to becoming trapped in local minimum.

Initially, a variable matrix including all the variable values was constructed systematically. Subsequently, MATLAB was utilized to rapidly communicate with Aspen, enabling the effective identification of variable combinations that ensure process convergence. Finally, the TAC of each process associated with the identified variable combinations was evaluated systematically. For EtOH/water feed molar ratios of 10/90, 30/70, 50/50, 70/30 and 90/10, the minimum TAC of LEDWC are 488007, 559093, 634546, 698340, and 742257 USD·a^{-1}, respectively; the minimum TAC of CED are 551823, 637197, 695667, 739048, and 754913 USD·a^{-1}, respectively.

Furthermore, this paper explores the mechanism behind the generation of local optima from the perspective of variable coupling and the flow behavior inside the column. Taking N_{CL} as an example for structural variables, as N_{CL} increases, the opposing effects between the decrease in RR_{CL} and the increase in reboiler temperature due to column pressure drop and changes in the bottom product lead to fluctuations in energy consumption, thereby inducing the emergence of local optima. For process variables, taking D_{CL} as an example, as it increases, RR_{CL} shows an upward trend to meet separation requirements; simultaneously, to ensure process convergence, D_L is adjusted within a certain range, with its changes showing no obvious pattern, further complicating the system response. These nonlinear interactions reinforce the coupling relationship between structural and process variables, ultimately resulting in multiple local minima in the TAC curve. Compared with CED, LEDWC has fewer local minima in the TAC and N_{CL} curves. Analysis of the flow characteristics inside the column revealed that CED exhibited obvious back-mixing, while LEDWC did not exhibit similar phenomena. This reduces the coupling effects between variables in LEDWC, thereby decreasing the probability of local optima occurring.

In conclusion, this study effectively solves the issue of local minimum by comprehensively exploring the solution, thereby improving the reliability of the optimization process. This approach enhances both the efficiency and accuracy of distillation optimization, while also offering valuable insights for tackling similar complex optimization challenges in chemical engineering. Moreover, this modular framework can be further integrated into meta-heuristic algorithms to accelerate convergence and enhance adaptability in future optimization tasks.

CRediT Authorship Contribution Statement

Chenghao Xing: Writing – original draft, Visualization, Supervision, Software, Methodology, Investigation, Conceptualization. Yanyang Wu: Writing – review & editing, Resources, Data curation, Conceptualization. Xiaolong Zhou: Writing – review & editing, Resources, Conceptualization. Bin Wu: Writing – review & editing, Methodology. Kui Chen: Investigation, Data curation. Lijun Ji: Validation, Data curation.

Declaration of Competing Interest

The authors declare that they have no known competing financial interests or personal relationships that could have appeared to influence the work reported in this paper.

Nomenclature

D_{CL}	distillation flow rate for CL, kmol·h^{-1}
D_{CR}	distillation flow rate for CR, kmol·h^{-1}
D_{EDC}	distillation flow rate for EDC, kmol·h^{-1}
D_{ERC}	distillation flow rate for ERC, kmol·h^{-1}
D_L	liquid stream flow rate between CL and CR, kmol·h^{-1}
$F_{S\text{-}CED}$	entrainer flow rate for CED, kmol·h^{-1}
$F_{S\text{-}LEDWC}$	entrainer flow rate for LEDWC, kmol·h^{-1}
N_{CL}	total number of stages for CL
N_{CR}	total number of stages for CR
N_{EDC}	total number of stages for EDC
N_{ERC}	total number of stages for ERC
$N_{F\text{-}CL}$	feed stage for CL
$N_{F\text{-}CR}$	feed stage for CR
$N_{F\text{-}EDC}$	feed stage for EDC
$N_{F\text{-}ERC}$	feed stage for ERC
$N_{F\text{-}E\text{-}CL}$	entrainer stage for CL
$N_{F\text{-}E\text{-}EDC}$	entrainer stage for EDC
$N_{F\text{-}L\text{-}CL}$	liquid stream withdrawal stage for CL
RR_{CL}	reflux ratio for CL
RR_{CR}	reflux ratio for CR
RR_{EDC}	reflux ratio for EDC
RR_{ERC}	reflux ratio for ERC

Supplementary Material

Supplementary data to this article can be found online at https://doi.org/10.1016/j.cjche.2025.09.020.

References

[1] Z. Ding, H.H. Zhang, H. Li, J.Y. Chen, P. Lu, C. Hua, Improved harmony search algorithm for enhancing efficiency and quality in optimization of the distillation process, *ACS Omega* 8 (31) (2023) 28487–28498.
[2] H.G. Silva, R.R. Salcedo, SIMOP: application to global MINLP stochastic optimization, *Chem. Eng. Sci.* 66 (6) (2011) 1306–1321.
[3] H.H. Zhang, P. Lu, Z. Ding, Y.B. Li, H. Li, C. Hua, Z. Wu, Design optimization and control of dividing wall column for purification of trichlorosilane, *Chem. Eng. Sci.* 257 (2022) 117716.
[4] C.H. Xing, Z.W. Song, Y.Y. Wu, B. Wu, K. Chen, L.J. Ji, Energy, exergy, economic, and environmental analysis of the vapor recompression-assisted liquid-only transfer extractive dividing wall column for separating minimum-boiling point azeotropes, *Ind. Eng. Chem. Res.* 63 (15) (2024) 6725–6742.
[5] J.L. Yan, J.Y. Liu, J.Y. Ren, Y. Wu, X.N. Li, T. Sun, L.Y. Sun, Design and multi-objective optimization of hybrid reactive-extractive distillation process for separating wastewater containing benzene and isopropanol, *Sep. Purif. Technol.* 290 (2022) 120915.
[6] Y. Yuan, X.Y. Tao, K.J. Huang, H.S. Chen, X. Qian, L. Zhang, Multi-objective optimization and composition control of Sargent dividing-wall distillation columns, *J. Clean. Prod.* 423 (2023) 138637.
[7] P.Z. Cui, F. Zhao, D. Yao, Z.Y. Ma, S.H. Li, X. Li, L. Wang, Z.Y. Zhu, Y.L. Wang, Y. X. Ma, D.M. Xu, Energy-saving exploration of mixed solvent extractive distillation combined with thermal coupling or heat pump technology for the separation of an azeotrope containing low-carbon alcohol, *Ind. Eng. Chem. Res.* 59 (29) (2020) 13204–13219.
[8] Y.N. Li, B.J. Huo, Z.F. Xu, H.Q. Qi, X. Li, P.Z. Cui, Z.Y. Zhu, Y.L. Wang, J.W. Yang, J. Gao, Energy-saving and environmentally friendly pervaporation-distillation hybrid process for alcohol and ester recovery from wastewater containing three binary azeotropes, *Sep. Purif. Technol.* 281 (2022) 119889.
[9] Z.Q. Liu, X.Y. Zhao, J.K. Zhang, Z.Z. Du, J.H. Wang, Optimization of EB/SM distillation processes based on divided wall columns in a PO/SM process with a chaos differential evolution algorithm, *ACS Omega* 7 (6) (2022) 5471–5484.
[10] Q.T. He, Q. Li, Y.F. Tan, L.C. Dong, Z.M. Feng, Multi-objective optimization of sustainable extractive dividing-wall column process for separating methanol and trimethoxysilane azeotrope mixture, *Chem. Eng. Process. Process Intensif.* 181 (2022) 109141.
[11] Y.J. Ma, N. Zhang, J. Li, C.W. Cao, Optimal design of extractive dividing-wall column using an efficient equation-oriented approach, *Front. Chem. Sci. Eng.* 15 (1) (2021) 72–89.
[12] A. Ramírez, J.R. Romero, C. García-Martínez, S. Ventura, JCLEC-MO: a Java suite for solving many-objective optimization engineering problems, *Eng. Appl. Artif. Intell.* 81 (2019) 14–28.

[13] T. Cai, S.S. Zhang, Z.W. Ye, W. Zhou, M.W. Wang, Q.Y. He, Z.Y. Chen, W.F. Bai, Cooperative metaheuristic algorithm for global optimization and engineering problems inspired by heterosis theory, *Sci. Rep.* 14 (1) (2024) 28876.
[14] A.G. Beck, S. Iyer, J. Fine, G. Chopra, Paddy: an evolutionary optimization algorithm for chemical systems and spaces, *Dig. Dis.* 4 (5) (2025) 1352−1371.
[15] I.E. Grossmann, Review of nonlinear mixed-integer and disjunctive programming techniques, *Optim. Eng.* 3 (3) (2002) 227−252.
[16] C.A. Floudas, C.E. Gounaris, A review of recent advances in global optimization, *J. Global Optim.* 45 (1) (2009) 3−38.
[17] A.A. Kiss, D.J.P.C. Suszwalak, Efficient bioethanol dehydration in azeotropic and extractive dividing-wall columns, *Procedia Eng.* 42 (2012) 566−572.
[18] H. Luo, C.S. Bildea, A.A. Kiss, Novel heat-pump-assisted extractive distillation for bioethanol purification, *Ind. Eng. Chem. Res.* 54 (7) (2015) 2208−2213.
[19] L.C. Nhien, N. Agarwal, M. Lee, Dehydration of isopropanol: a comparative review of distillation processes, heat integration, and intensification techniques, *Energies* 16 (16) (2023) 5934.
[20] Ş.İ. Kırbaşlar, S. Şahin, M. Bilgin, (Liquid + liquid) equilibria of (water + butyric acid + dibasic esters) ternary systems, *J. Chem. Thermodyn.* 39 (2) (2007) 284−290.
[21] L.A. Onuchak, R.F. Stepanova, S.Y. Kudryashov, O.B. Akopova, The thermodynamic parameters of sorption and selectivity of chiral nematic liquid crystals of terephthalidene-bis-2-methylbutyl para-aminobenzoate, *Russ. J. Phys. Chem. A* 82 (2) (2008) 269−275.
[22] N.V. Lifanova, T.M. Usacheva, M.V. Zhuravlev, Equilibrium and relaxation dielectric properties of 1,2-ethanediol, *Russ. J. Phys. Chem. A* 81 (5) (2007) 820−828.
[23] H.S. Lai, Y.F. Lin, C.H. Tu, Isobaric (vapor + liquid) equilibria for the ternary system of (ethanol + water + 1,3-propanediol) and three constituent binary systems at $P = 101.3$ kPa, *J. Chem. Thermodyn.* 68 (2014) 13−19.
[24] N. Kamihama, H. Matsuda, K. Kurihara, K. Tochigi, S. Oba, Isobaric vapor−liquid equilibria for ethanol + water + ethylene glycol and its constituent three binary systems, *J. Chem. Eng. Data* 57 (2) (2012) 339−344.
[25] J.D. Li, C.X. Chen, J. Wang, Vapor−liquid equilibrium data and their correlation for binary systems consisting of ethanol, 2-propanol, 1,2-ethanediol and methyl benzoate, *Fluid Phase Equilib.* 169 (1) (2000) 75−84.
[26] J.M. Douglas, Conceptual Design of Chemical Processes, McGraw-ill, NY (1988).
[27] Z.H. Si, H. Chen, H.F. Cong, X.G. Li, Energy, exergy, economic and environmental analysis of a novel steam-driven vapor recompression and organic Rankine cycle intensified dividing wall column, *Sep. Purif. Technol.* 295 (2022) 121285.
[28] Z.W. Song, W. Cui, Y.Y. Wu, B. Wu, K. Chen, L.J. Ji, Energy, exergy, economic, and environmental analysis of a novel liquid-only transfer dividing wall column with vapor recompression, *Sep. Purif. Technol.* 329 (2024) 125122.
[29] A.A. Kiss, Advanced Distillation Technologies: Design, Control, and Applications, Wiley, Chichester, United Kingdom (2013).
[30] C.T. Cui, X.G. Li, D.R. Guo, J.S. Sun, Towards energy efficient styrene distillation scheme: from grassroots design to retrofit, *Energy* 134 (2017) 193−205.
[31] G.M. Cordeiro, M.F. de Figueirêdo, W.B. Ramos, F.A. Sales, K.D. Brito, R.P. Brito, Systematic strategy for obtaining a dividing-wall column applied to an extractive distillation process, *Ind. Eng. Chem. Res.* 56 (14) (2017) 4083−4094.